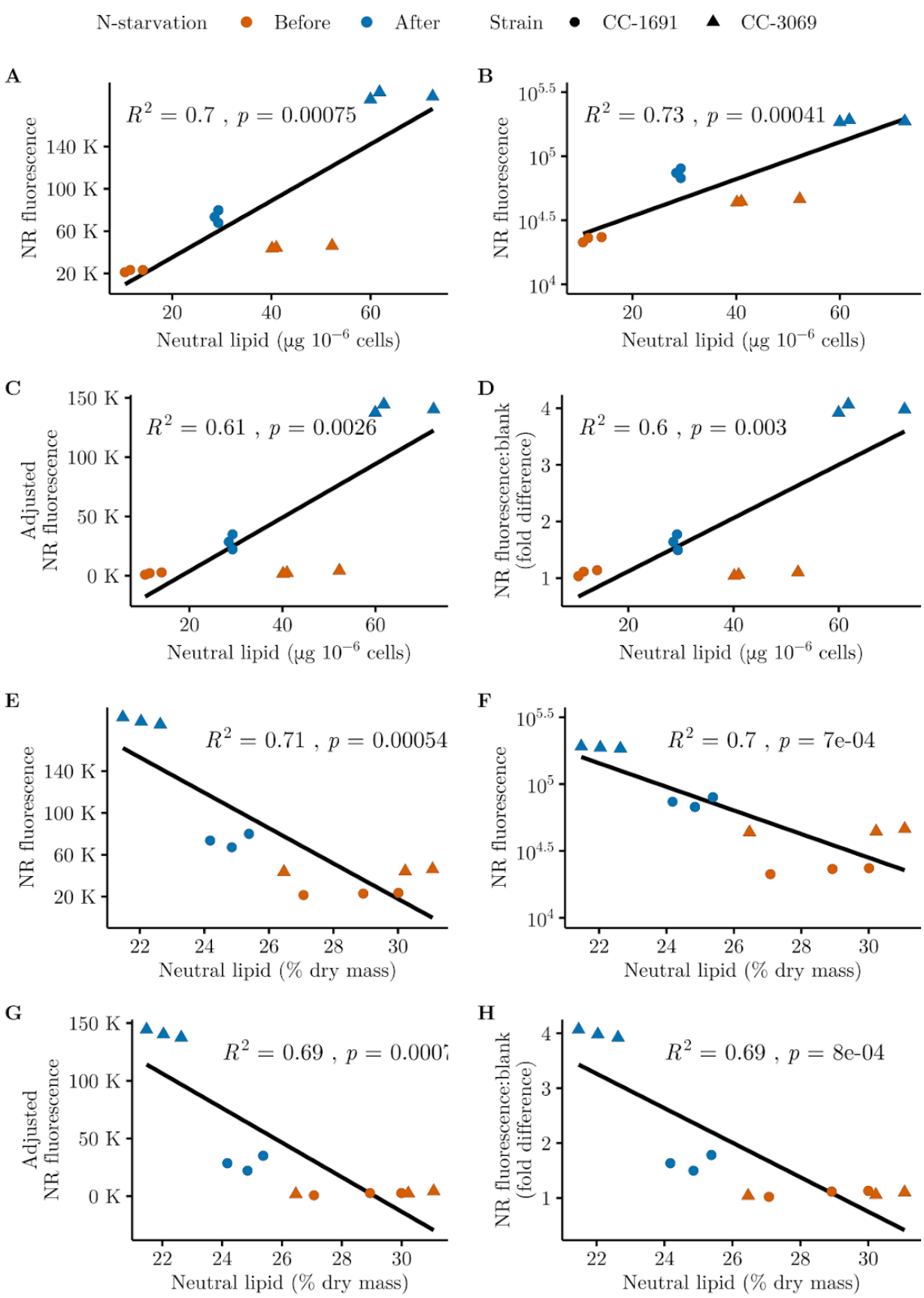
N-starvation
Before
After
Strain
CC-1691
CC-3069
A
$R^2 = 0.7$, $p = 0.00075$
NR fluorescence
140 K
100 K
60 K
20 K
20
40
60
Neutral lipid (µg 10^{-6} cells)
B
$R^2 = 0.73$, $p = 0.00041$
NR fluorescence
$10^{5.5}$
10^{5}
$10^{4.5}$
10^{4}
20
40
60
Neutral lipid (µg 10^{-6} cells)
C
$R^2 = 0.61$, $p = 0.0026$
Adjusted NR fluorescence
150 K
100 K
50 K
0 K
20
40
60
Neutral lipid (µg 10^{-6} cells)
D
$R^2 = 0.6$, $p = 0.003$
NR fluorescence:blank (fold difference)
4
3
2
1
20
40
60
Neutral lipid (µg 10^{-6} cells)
E
$R^2 = 0.71$, $p = 0.00054$
NR fluorescence
140 K
100 K
60 K
20 K
22
24
26
28
30
Neutral lipid (% dry mass)
F
$R^2 = 0.7$, $p = 7e\text{-}04$
NR fluorescence
$10^{5.5}$
10^{5}
$10^{4.5}$
10^{4}
22
24
26
28
30
Neutral lipid (% dry mass)
G
$R^2 = 0.69$, $p = 0.000$
Adjusted NR fluorescence
150 K
100 K
50 K
0 K
22
24
26
28
30
Neutral lipid (% dry mass)
H
$R^2 = 0.69$, $p = 8e\text{-}04$
NR fluorescence:blank (fold difference)
4
3
2
1
22
24
26
28
30
Neutral lipid (% dry mass)

Figure 3. NR calibration curves of *C. reinhardtii* CC-1691 and CC-3069 using all combinations of NR fluorescence and neutral lipid content metrics (α=0.00625). Flask cultures of CC-1691 and CC-3069 are sampled in triplicates before and 3-days after N-starvation treatment (n=12 flasks).

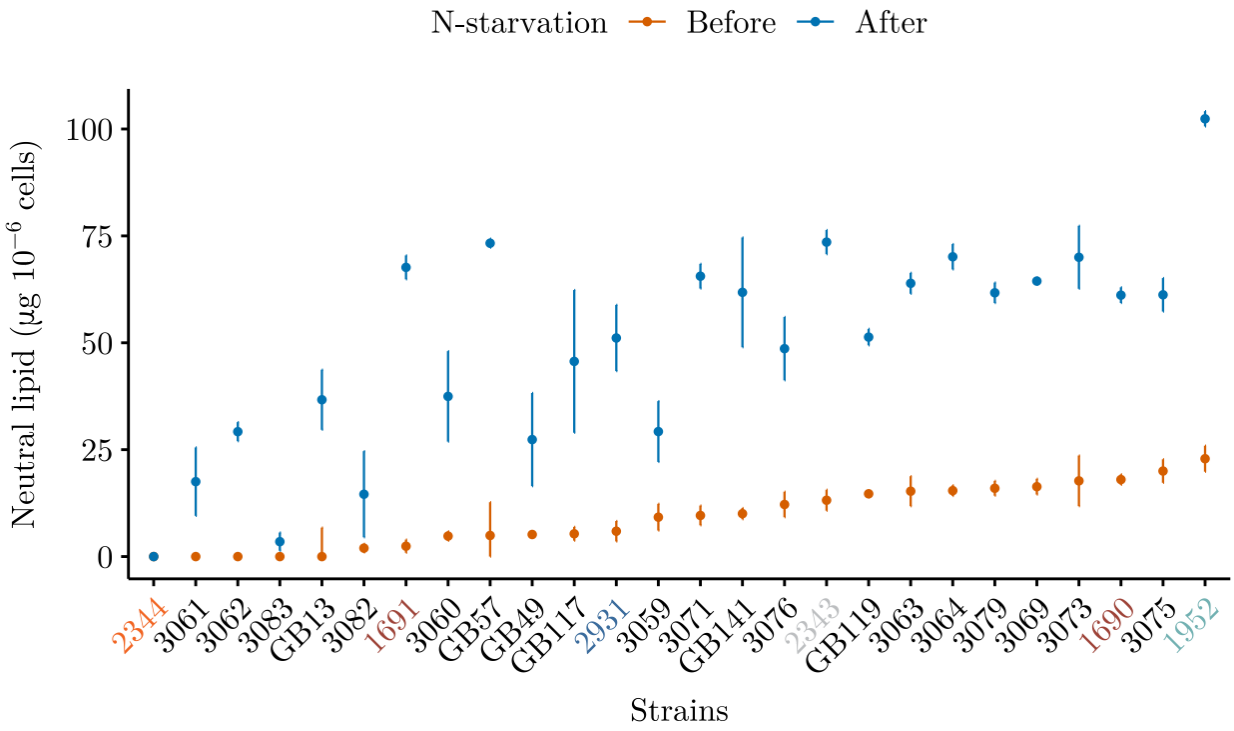

Figure 4. Variation of predicted neutral lipid content among 26 natural populations of C. *reinhardtii*. Strains are ordered by the magnitude of neutral lipid content before N-starvation and strain labels are colored by geographical origins (**Figure 1**). Each point represents the mean predicted neutral lipid content across three replicates within each Strain × N-Starvation combination. Error bars are the standard errors across three replicates. The neutral lipid content is predicted using measured NR fluorescence (**Figure S9**) and the calibration curve (**Figure 3B**).

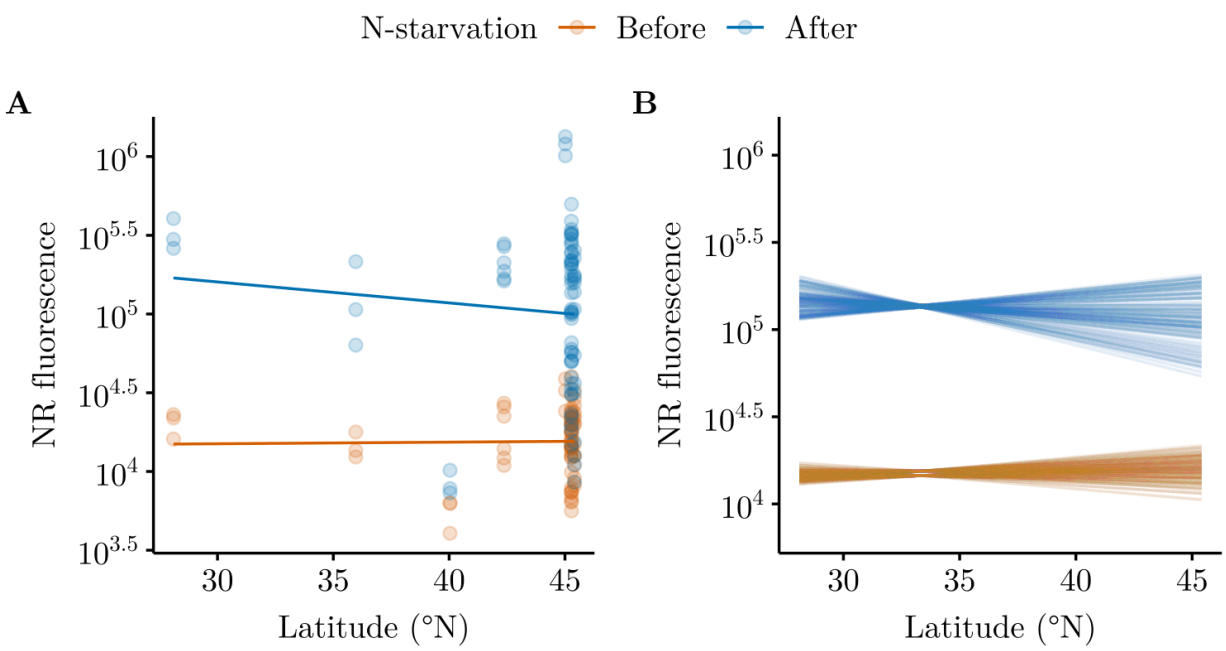

Figure 5. Latitudinal variation of neutral lipid content in 26 *C. reinhardtii* strains. (A) Each point represents the NR fluorescence of each replicate, and the regression line shows the linear correlation between NR fluorescence and latitude within each N-starvation treatment. (B) Downsampled regressions of neutral lipid content across latitudes (n=10,000 runs).

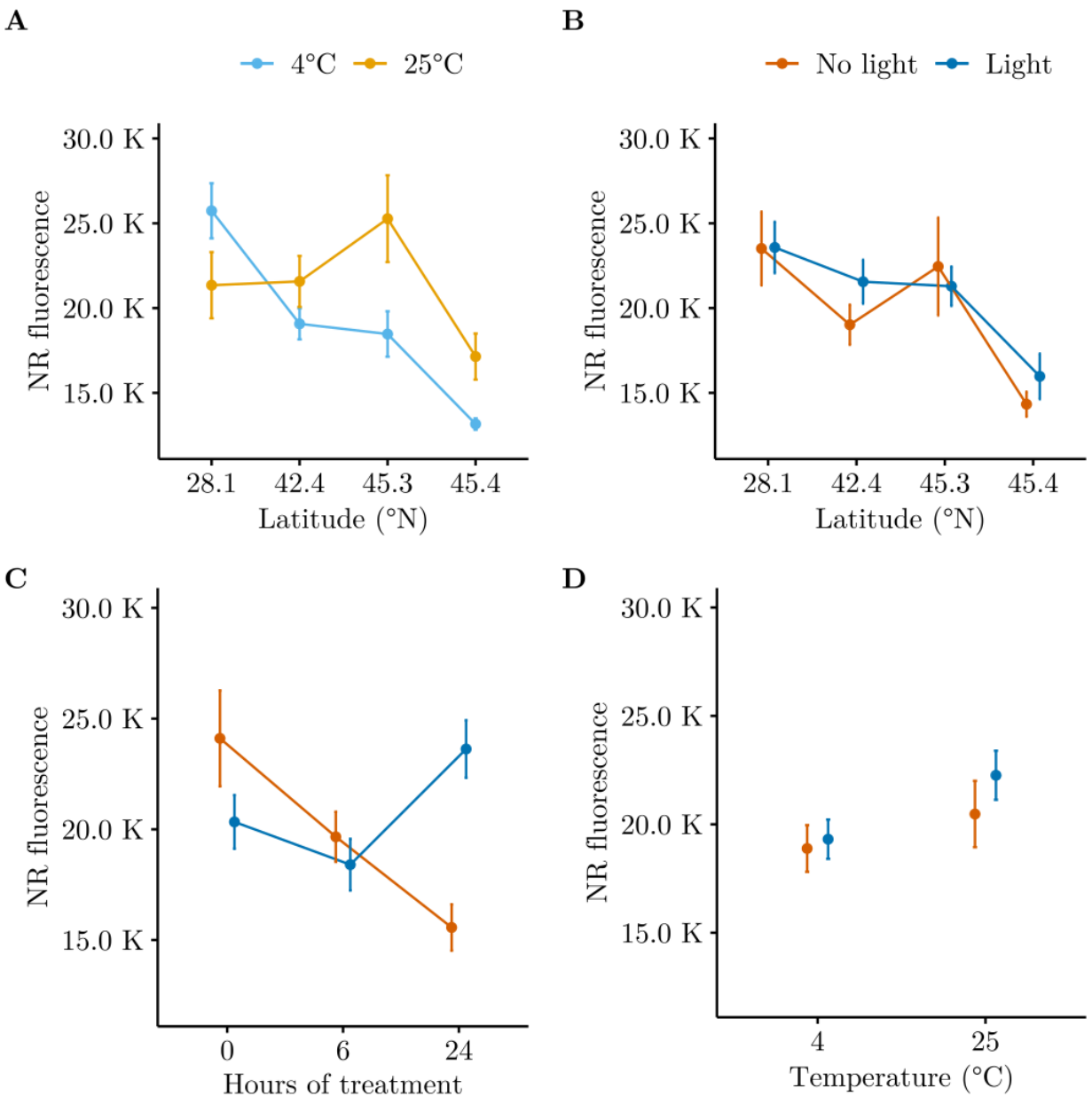

Figure 6. The effect of light, temperature, and latitude on neutral lipid accumulation in five *C. reinhardtii* strains. Error bars represent the standard error of the replicates in each treatment combination.

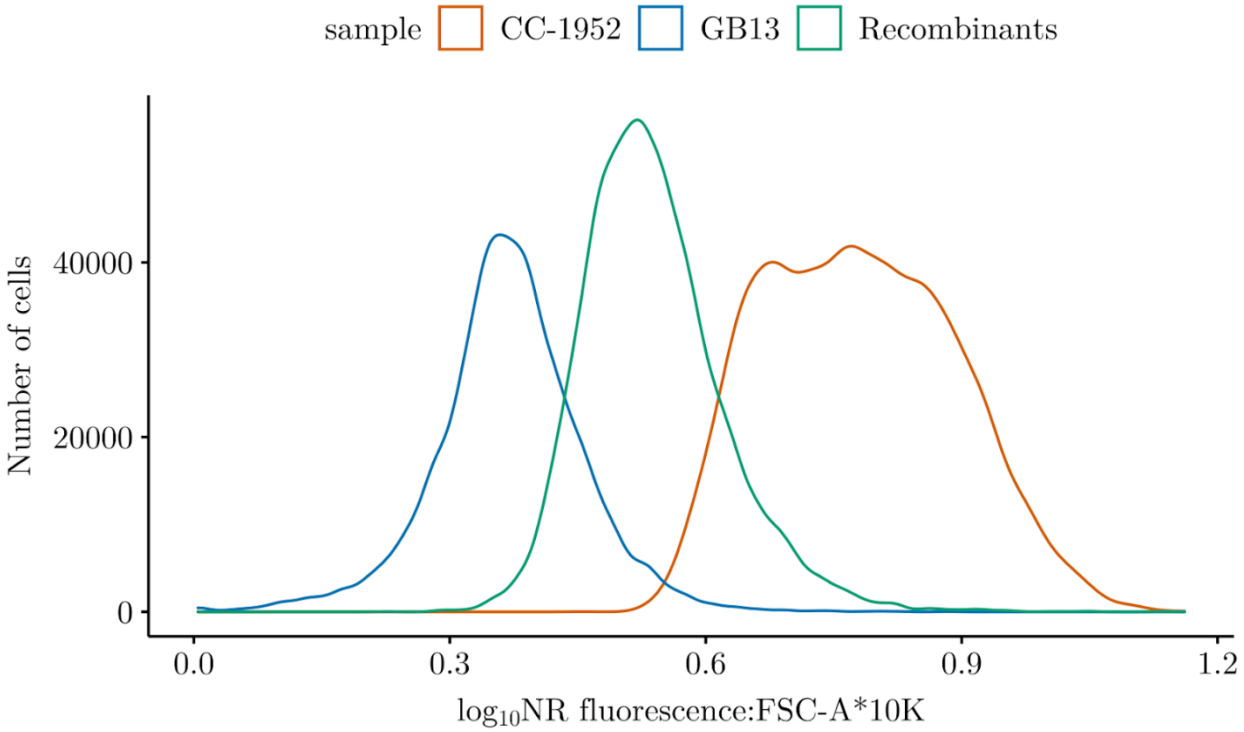

Figure 7. The distribution of NR fluorescence for CC-1952, GB-13 and their recombinants. Each distribution is plotted from the flow cytometric measurements of one replicate (n=1) for each strain.

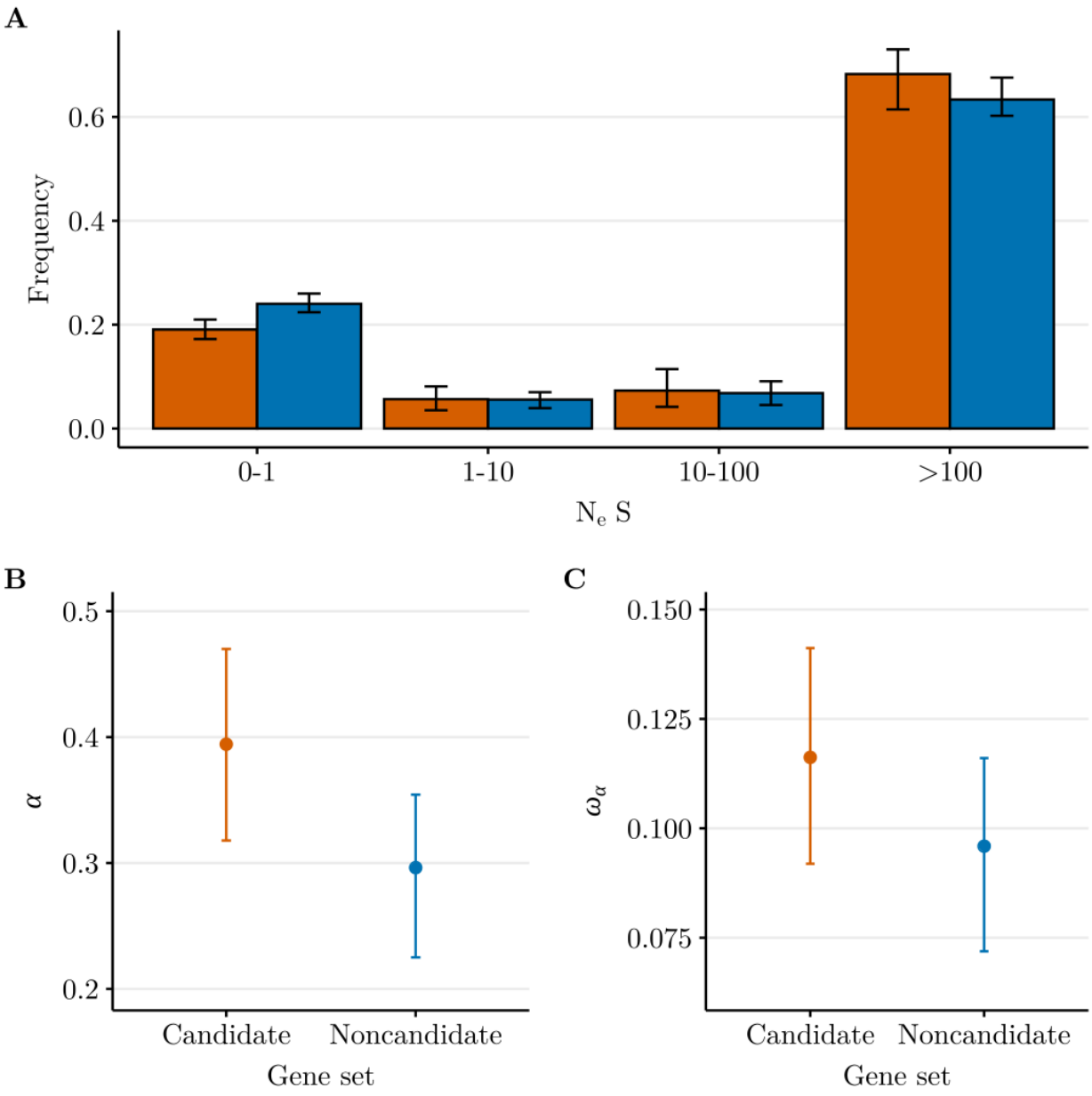

Figure 8. The distribution of fitness effects (DFE) of candidate and noncandidate genes associated with lipid accumulation in *C. reinhardtii*. N_eS is the product of effective population size (N_e) and the strength of selection (S). The DFE is estimated using bootstraps of site frequency spectra of 473 candidate genes and 11800 noncandidate genes. (A) Frequency is the proportion of mutations expected to fall into each selection regime. (B) *a* is the proportion of non-synonymous changes that were driven by adaptive substitutions, and (C) ω_α is the rate of adaptive substitution measured relative to neutral substitution.